

Supporting Information

Preparation of PCDTBT Nanofibers with Diameter of 20 nm and Their Application to Air-Processed Organic Solar Cells

*Taehoon Kim, Seung Jae Yang, Sung Kyun Kim, Hong Soo Choi, and Chong Rae Park**

Carbon Nanomaterials Design Laboratory, Global Research Laboratory, Research Institute of Advanced Materials, and Department of Materials Science and Engineering, Seoul National University, Seoul 151-744, Korea

Preparation of the PCDTBT nanofibers

Previous efforts toward developing OPV devices using electrospinning techniques have explored the use of P3HT:PCBM fibers as an active layer¹ or metal oxide nanofibers as an electron acceptor.^{2, 3} The preparation of an electron donor layer using electrospinning techniques has not yet been investigated because fiber diameters on the scale of the exciton diffusion length had not previously been achieved. The performance of the P3HT:PCBM fibers in the active layer was not significantly influenced by the fiber diameter because these fibers formed a bulk heterojunction structure, the function of which did not significantly depend on the fiber diameter. Metal oxide precursors are readily dissolved in polar solvents with a high electrical conductivity to facilitate the preparation of nanofibers; however, conjugated polymer nanofibers with diameters comparable to the exciton diffusion length cannot be prepared using chlorinated solvents with a low conductivity because the conjugated polymers display a low solubility in such solvents. We previously reported a method of preparing P3HT and F8BT nanofibers.⁴ The viscosity or electric conductivity of the spinning dope solution could be tuned by adding an auxiliary polymer or a polar solvent, respectively. Earlier results indicated that the diameter and morphology of the PCDTBT@PEO nanofibers could be optimized. Since the auxiliary polymer must be removed prior to incorporation into the active layer, the amount of auxiliary polymer added should be minimized as long as beads do not form. Figure S1 shows SEM images of the PCDTBT@PEO nanofibers electrospun from different spinning dope solutions. The concentration ratio of the PCDTBT was fixed at 0.1 wt% because the solubility of the PCDTBT was low in this solution. A 0.4 wt% PEO concentration clearly induced the generation of beads on the electrospun fibers. The low viscosity of the 0.4 wt% PEO spinning dope solution (Figure S2) was known to be inappropriate for electrospinning, but the highly volatile chloroform appeared to form

nanofibers without generating beads.⁵

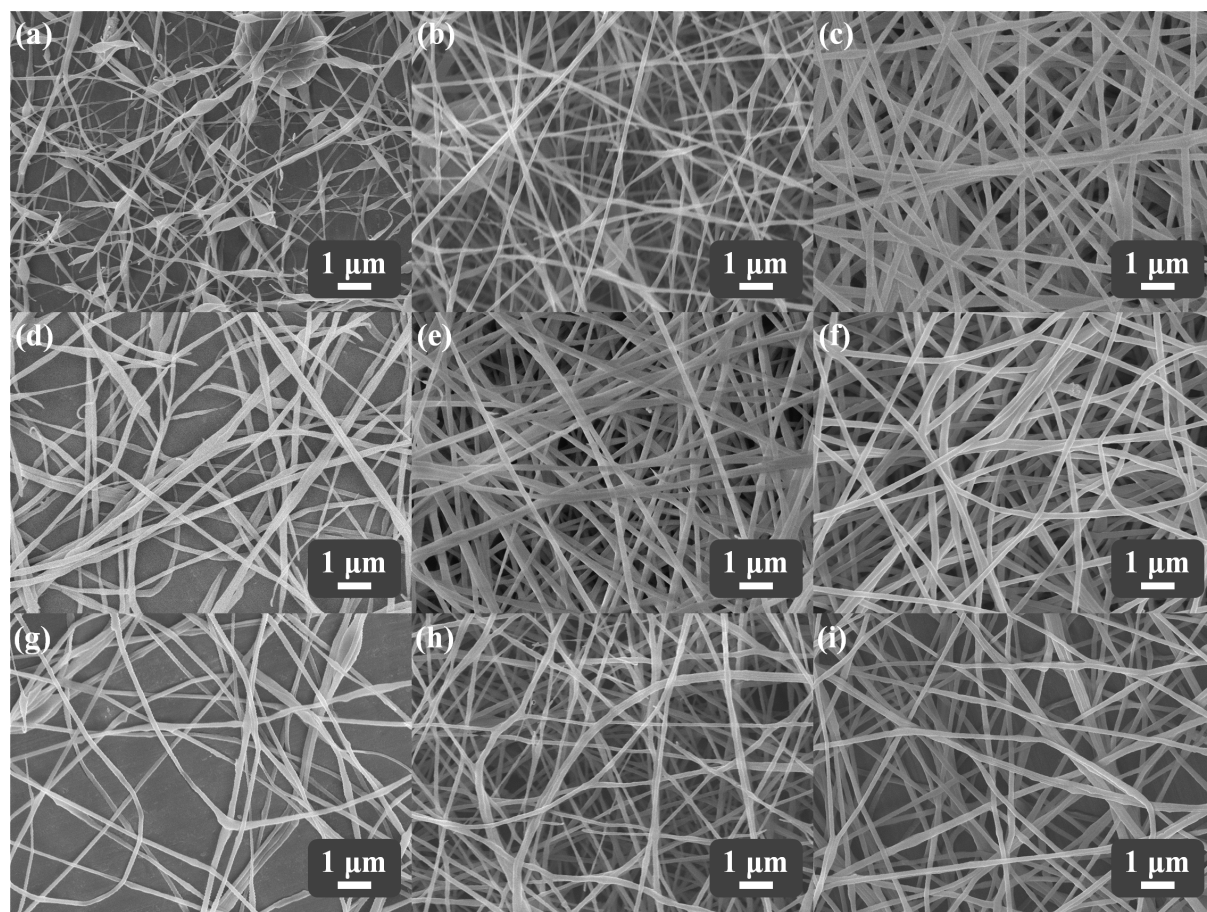


Figure S1. SEM micrographs of the electrospun PCDTBT@PEO nanofibers prepared from solutions containing various concentrations of the polar solvents and PEO. The concentrations of PEO were 0.3 wt% (a, d, g), 0.4 wt% (b, e, h), and 0.5 wt% (c, f, i). The chloroform:polar solvent ratios were 10:1 (w/w) (a, b, c), 8:1 (d, e, f), and 6:1 (g, h, i).

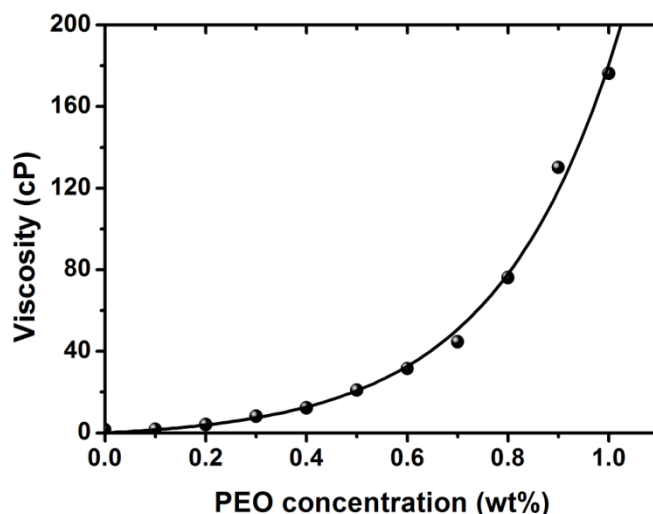


Figure S2. The viscosities of the spinning dope solutions.

The auxiliary polymer was removed from the PCDTBT@PEO composite nanofibers using acetonitrile due to its selective solubility for PEO. Previous reports⁴ indicated that isopropanol displayed the best performance with respect to PEO removal from the composite nanofibers; however, the PEO removal using isopropanol should be performed above 70°C, which can degrade the device. Acetonitrile could dissolve the high molecular weight PEO at room temperature, therefore, acetonitrile was employed in this experiment. The removal efficiency was increased by dipping the layer several times to prevent the re-adsorption of the dissolved auxiliary polymer from the dilute wash solution onto the PCDTBT fibers.⁶

The residue on the PCDTBT fibers was characterized by FT-IR and TGA. Because PEO fibers were completely degraded at 370°C (Figure S4), the PEO residue on the nanofibers could be calculated based on the thermal behavior of the electrospun PEO fibers and the electrosprayed conjugated polymer.⁶ The thermal behaviors of the virgin PCDTBT nanofibers were nearly identical to the behavior of PCDTBT (Figure S4), indicating that the PEO was nearly absent from the virgin PCDTBT nanofibers.

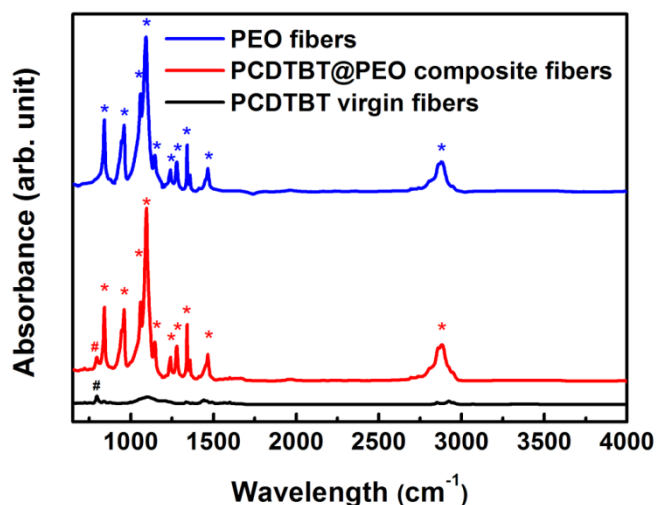


Figure S3. FT-IR spectra of electrospun PEO fibers, PCDTBT@PEO composite fibers and PCDTBT virgin fibers.

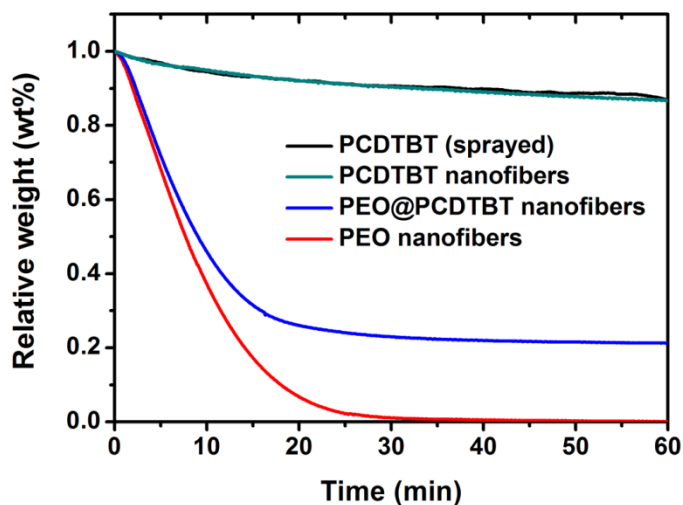


Figure S4. Thermogravimetric thermograms of the samples under isothermal treatment at 370°C.

The PCDTBT nanofiber diameter was directly related to the concentration of PCDTBT in the electrospinning solution. The electrospun fiber diameter was also influenced by the intensity of the stretching effects during electrospinning, as determined by the electrical conductivity and viscosity of the spinning dope solution. The PCDTBT nanofiber diameter could,

therefore, be tuned according to the concentration of PCDTBT, the viscosity, and the electrical conductivity of the spinning dope solution. The effects of the PCDTBT nanofiber diameter on the photovoltaic performance were investigated by preparing four PCDTBT nanofibers with different diameters: 50 nm, 120 nm, and 200 nm. The PCDTBT nanofibers were electrospun from different spinning dope solutions, as illustrated in Figure S5.

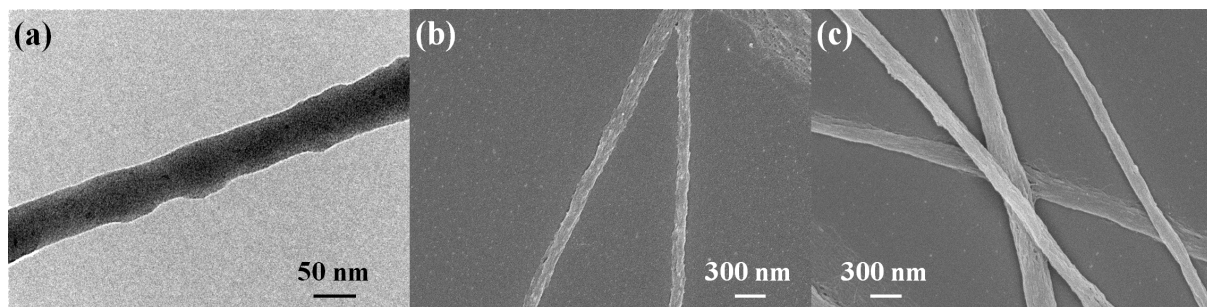


Figure S5. TEM micrographs of the virgin PCDTBT nanofibers with a diameter of (a) 50 nm, and SEM micrographs of virgin PCDTBT nanofibers with diameters of (b) 120 nm, and (c) 200 nm.

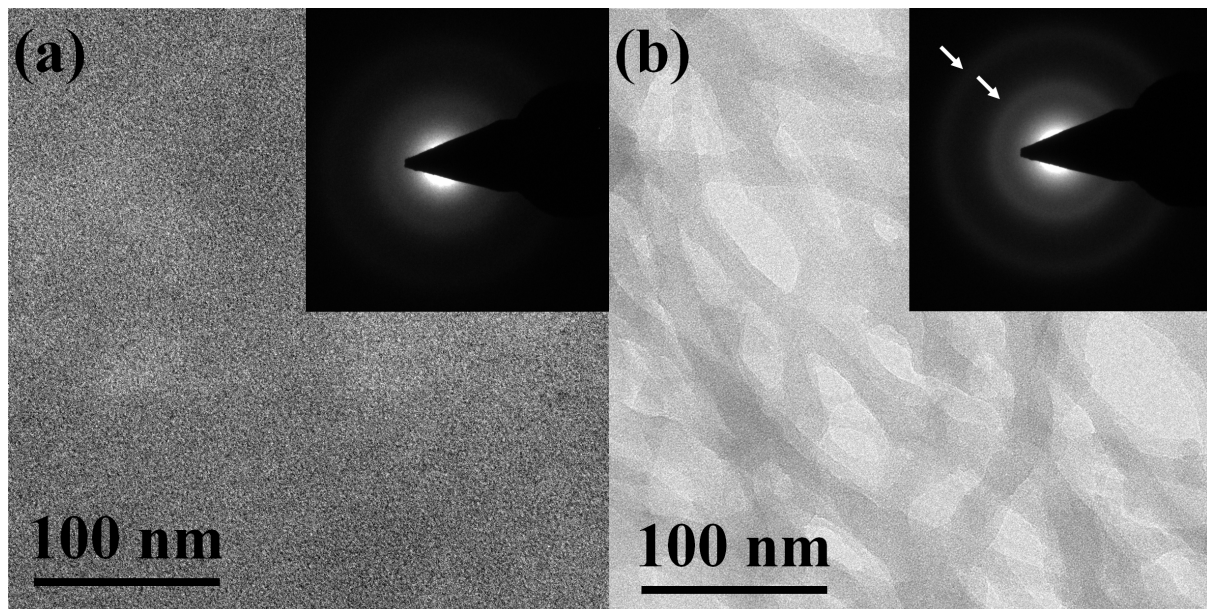


Figure S6. TEM micrographs of (a) PCDTBT film and (b) virgin PCDTBT nanofibers. The insets show the SAED patterns of the samples.

Photovoltaic performance

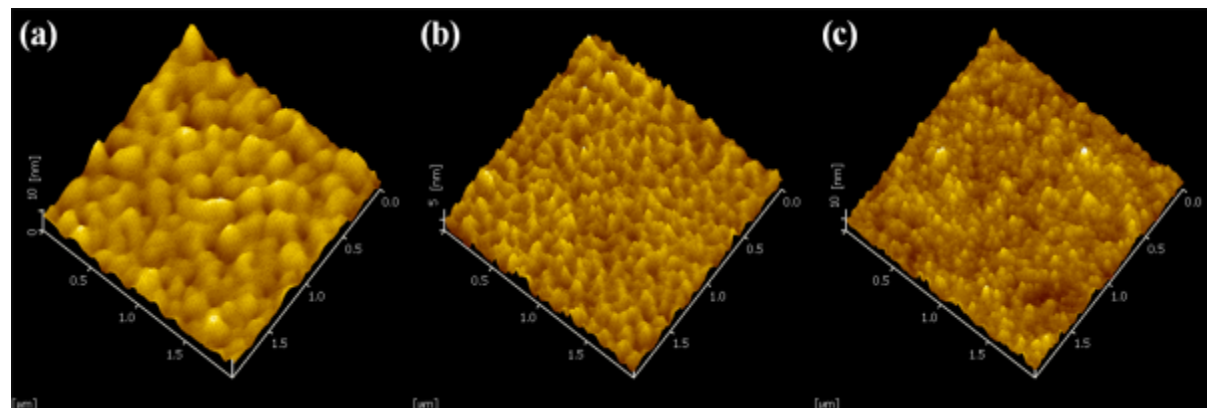


Figure S7. AFM images ($2 \mu\text{m} \times 2 \mu\text{m}$) of the (a) BHJ, (b) pseudo-bilayer, and (c) nanofibrous active layers composed of PCDTBT:PC₇₀BM.

Park et al. reported that the photocurrent of their OPV device flattened under reverse bias conditions because the internal quantum efficiency of the OPV device approached 100%.⁷ These results indicate that the OPV device had extracted the photogenerated charge under short circuit conditions. Consequently, no additional charges could be harvested, even under high reverse bias conditions. In view of these results, we tested our BHJ/pseudo-bilayer/nanofibrous OPV devices under reverse bias conditions to determine whether the nanofibers affected the charge collection. The photocurrent was obtained by subtracting the dark current from the light current to compensate for the diode. All three types of OPV devices showed flatter current densities below 0 V, but the current density slope for the nanofibrous OPV device was smaller than the slope for the BHJ device.

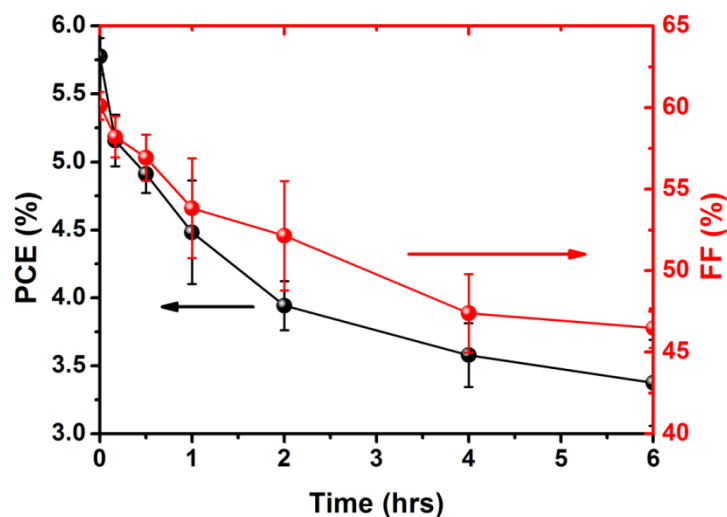


Figure S8. Device performance variation on the exposure time in ambient air.

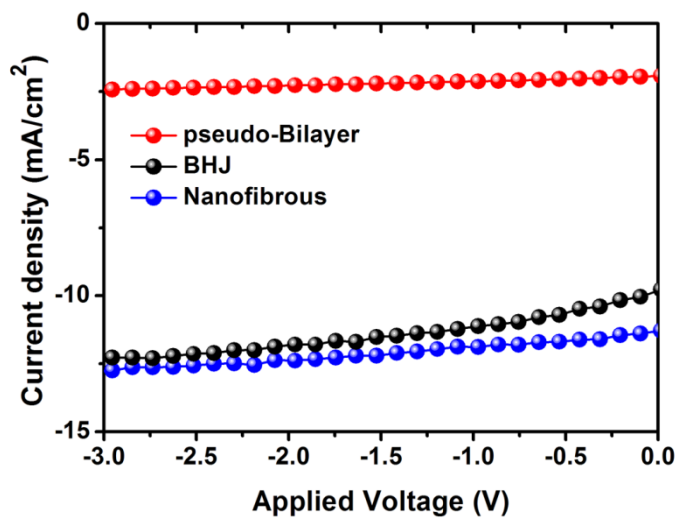


Figure S9. Calculated photocurrent density–voltage curves of the devices prepared using the PCDTBT:PC₇₀BM BHJ, pseudo-bilayer, and nanofibrous structures.

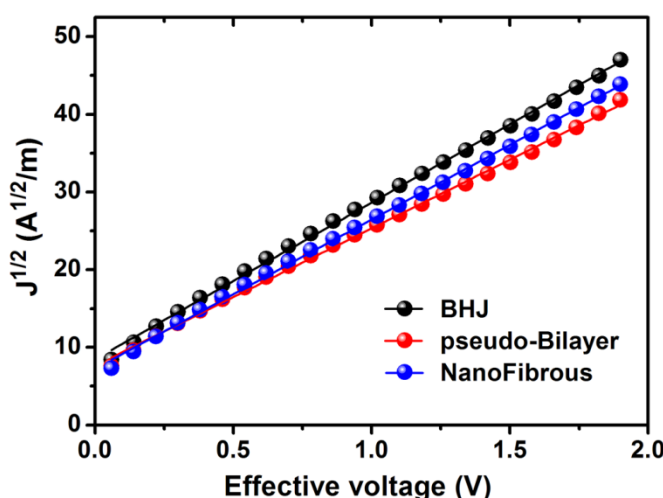


Figure S10. Dark $J^{1/2}$ -V characteristics for the SCLC hole-only devices prepared using the PCDTBT:PC₇₀BM BHJ, pseudo-bilayer, and nanofibrous structures..

References

1. N. M. Bedford, M. B. Dickerson, L. F. Drummy, H. Koerner, K. M. Singh, M. C. Vasudev, M. F. Durstock, R. R. Naik and A. J. Steckl, *Adv. Energy Mater.*, 2012, **2**, 1136-1144.
2. S. Wu, Q. Tai and F. Yan, *J. Phys. Chem. C*, 2010, **114**, 6197-6200.
3. H.-S. Shim, S.-I. Na, S. H. Nam, H.-J. Ahn, H. J. Kim, D.-Y. Kim and W. B. Kim, *Appl. Phys. Lett.*, 2008, **92**, 183107-183103.
4. T. Kim, J. H. Im, H. S. Choi, S. J. Yang, S. W. Kim and C. R. Park, *J. Mater. Chem.*, 2011, **21**, 14231-14239.
5. G. Eda and S. Shrivkumar, *J. Appl. Polym. Sci.*, 2007, **106**, 475-487.
6. S. E. Harton, J. Lüning, H. Betz and H. Ade, *Macromolecules*, 2006, **39**, 7729-7733.
7. S. H. Park, A. Roy, S. Beaupre, S. Cho, N. Coates, J. S. Moon, D. Moses, M. Leclerc, K. Lee and A. J. Heeger, *Nat. Photonics*, 2009, **3**, 297-303.